New approaches for achieving more perfect transition metal oxide thin films 🅕

J. L. MacManus-Driscoll, 🆔 Matthew P. Wells, Chao Yun, Jung-Woo Lee, Chang-Beom Eom, and 🆔 Darrell G. Schlom

COLLECTIONS

Paper published as part of the special topic on New Perspectives on Emerging Advanced Materials for Sustainability NPAMS2020

🅕   This paper was selected as Featured

open access

View Online   Export Citation   CrossMark

ARTICLES YOU MAY BE INTERESTED IN

Oxygen vacancies: The (in)visible friend of oxide electronics
Applied Physics Letters **116**, 120505 (2020); https://doi.org/10.1063/1.5143309

Aspects of the synthesis of thin film superconducting infinite-layer nickelates
APL Materials **8**, 041107 (2020); https://doi.org/10.1063/5.0005103

Strongly correlated and topological states in [111] grown transition metal oxide thin films and heterostructures
APL Materials **8**, 050904 (2020); https://doi.org/10.1063/5.0009092

New approaches for achieving more perfect transition metal oxide thin films ⒡

View Online   Export Citation   CrossMark

J. L. MacManus-Driscoll,[1] Matthew P. Wells,[1,a)] Ⓘ Chao Yun,[1] Jung-Woo Lee,[2] Chang-Beom Eom,[2] and Darrell G. Schlom[3,4] Ⓘ

AFFILIATIONS

[1] Department of Materials Science and Metallurgy, University of Cambridge, 27 Charles Babbage Rd., Cambridge CB3 0FS, United Kingdom
[2] Department of Materials Science and Engineering, University of Wisconsin-Madison, 1550 Engineering Drive, Madison, Wisconsin 53706, USA
[3] Department of Materials Science and Engineering, Cornell University, 230 Bard Hall, Ithaca, New York 14853-1501, USA
[4] Kavli Institute at Cornell for Nanoscale Science, Ithaca, New York 14853, USA

Note: This paper is part of the Special Issue on New Perspectives on Emerging Advanced Materials for Sustainability.
a) Author to whom correspondence should be addressed: mpw52@cam.ac.uk

ABSTRACT

This perspective considers the enormous promise of epitaxial functional transition metal oxide thin films for future applications in low power electronic and energy applications since they offer wide-ranging and highly tunable functionalities and multifunctionalities, unrivaled among other classes of materials. It also considers the great challenges that must be overcome for transition metal oxide thin films to meet what is needed in the application domain. These challenges arise from the presence of intrinsic defects and strain effects, which lead to extrinsic defects. Current conventional thin film deposition routes often cannot deliver the required perfection and performance. Since there is a strong link between the physical properties, defects and strain, routes to achieving more perfect materials need to be studied. Several emerging methods and modifications of current methods are presented and discussed. The reasons these methods better address the perfection challenge are considered and evaluated.

I. INTRODUCTION

Since the discovery of high-temperature superconductivity in perovskite oxides in 1986, the unearthing of a huge range of physical phenomena in transition-metal oxides (TMOs) has been nothing short of remarkable, e.g., new magnetics, ferroelectrics, multiferroics, semiconductors, transparent conductors, calorics, plasmonics, catalysts, and ionic conductors, particularly from prominent solid state chemistry groups, e.g., Refs. 1–6. Most of the efforts have been focused on perovskites because these systems exhibit the widest range of highly tunable properties. However, it has been a great challenge for materials scientists to take the bulk phenomena of perovskites and translate these to thin films for electronic and energy applications, where very many potential applications exist (Fig. 1). Owing to the different nature of thin films vs bulk

growth, thin films are more defective than bulk.[7–11] On the other hand, advances in growth techniques have been impressive,[12,13] enabling new phenomena to be discovered, e.g., emergent effects at interfaces.[14]

While much work on TMO perovskite thin films is motivated by the search for a replacement for silicon as we near the end of Moore's law, there are very many other electronic and energy applications. Indeed, the very urgent need to reduce power consumption to slow global warming makes TMO devices, with their unrivaled stability, all-encompassing properties, in most cases low toxicity, and ability to be made in large areas, of unprecedented importance. For this reason, a paradigm shift in thinking is needed to put funding of materials engineering of TMO films on, at the very least, an equal footing with the basic science funding.
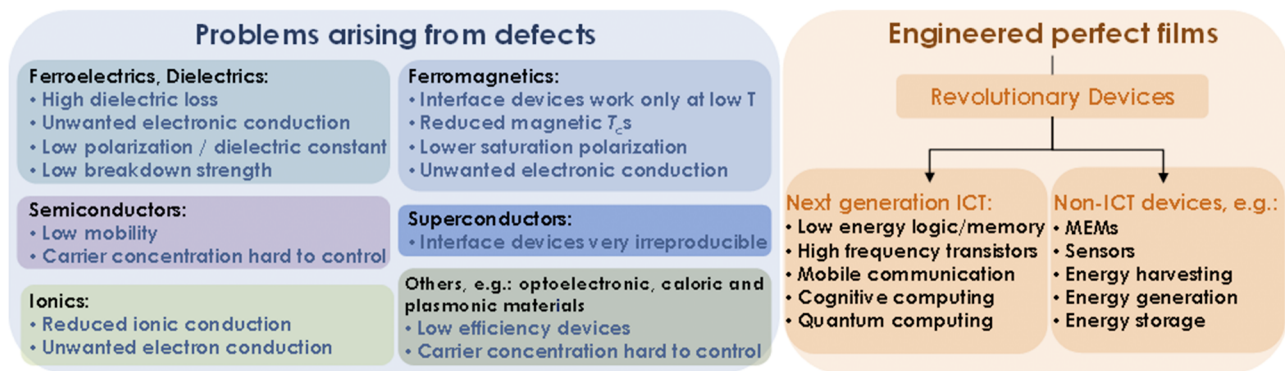
FIG. 1. The defect problem of oxide thin films and devices which would emerge if epitaxial films could be made with very high perfection.

A key challenge for TMO thin films is their high defect concentrations, which are significantly greater than in conventional semiconductors. The defects lead to degraded properties (Fig. 1), and so our ability both to fully understand the fascinating properties of oxides and to realize applications has been hampered. Defects cannot necessarily be overcome using standard growth tools. Considering the very wide application horizon (Fig. 1), new thinking in ways to make more perfect epitaxial complex oxide thin films is urgently needed. Hence, just as conventional semiconductors required precision materials engineering to transition from scientific curiosity to a $>400 \times 10^9$ dollar per year industry,[15] so do oxides.

So why do we have this problem? In fact, complex TMOs are complex, just as their name suggests, much more so than standard semiconductors: they have strongly correlated properties, strong Coulombic interactions,[16] and variable cation valence states. We note that oxide thin films *without* variable cation valence states, such as Ga_2O_3 and InGaZnO, which find wide-ranging applications today in photodetectors, photovoltaics, and thin film transistors,[17–19] are much more controllable systems. The question is how to achieve controlled properties in mixed valence cation TMOs. Clearly, control of their perfection is acute. Point defects arise because films are grown far below their melting points and because defect formation energies are low, typically lower than in standard semiconductors.[20,21] In elemental semiconductors, such as Si and Ge, the major source of point defects is impurities. The development of zone refining has produced ultra-pure semiconductor materials and has allowed exquisite control of n-type and p-type regions by adding small amounts of impurities, which directly impact device performance.[22] In compound semiconductors such as GaAs, the impurities play a critical role in determining electron mobility.[23] In the case of TMOs, however, both anion and cation non-stoichiometry is the key challenge, rather than the purity of materials.

II. DEFECTS IN TRANSITION METAL OXIDE FILMS IN RELATION TO STOICHIOMETRY CONTROL

From thermodynamic considerations, all compounds sustain a degree of intrinsic non-stoichiometry. The case of oxides is well documented.[24] For TMOs, under equilibrium conditions, there are variations in

1. *Oxygen composition.* Oxygen vacancies can readily form, depending on the oxide in question, as well as the formation of pO_2 and temperature. The oxygen vacancies will either induce a change in the electron concentration or the average TM valence or both. In a perfect system, oxygen vacancies can be filled by appropriate annealing at temperatures where the diffusivities are sufficiently high under pO_2s, which ensure that oxygen uptake is thermodynamically preferable.

2. *Cation composition and mixed valence cations.* The oxidation conditions strongly influence not only the oxygen stoichiometry but also the cation stoichiometry. If the growth conditions are too oxidizing, cation defects readily form, as binary oxide second phases become stable, and the perovskite becomes cation deficient.[25] TM cation vacancies and redox reactions leading to mixed valence TM cations cause modified physical properties and hard-to-control electronic conduction. Uncontrollable electronic conduction, even at a low level, is a very serious problem for mixed-valence TMO systems, which rely on achieving very low carrier concentrations, namely, ferroelectrics, dielectrics, ionics, and insulators. Anneals at temperatures of ~0.7×, the melting temperature is needed for recrystallization (and hence for cation vacancies to be removed).[26] However, since the melting points of strongly correlated TMOs are typically over ~1500 °C, for thin films such anneals are mostly impractical.

Since high temperature post-anneals are impractical, the best way to prevent cation defects from forming is to use lower oxidation conditions *during growth*. Such lower oxidation may lead to reduced oxygen concentration in the film, but this is remedied by an oxidizing post-anneal *after growth* to give full oxygen stoichiometry. Using such an approach, optimum physical properties have been achieved in (La, Sr)MnO_3 and $BiFeO_3$.[27,28] We note that the non-TMO perovskites, e.g., $BaSnO_3$, are less susceptible to variable electronic conduction from cation defects since mixed valence of the non-TMO cations is less prevalent

and any n-type defects are completely compensated by acceptor defects.[29]

III. TYPICAL GROWTH METHODS FOR HIGH QUALITY TRANSITION METAL OXIDE FILMS

Pulsed laser deposition (PLD) is a versatile growth technique to grow TMOs because of its ability to transfer the composition of the target materials into thin films.[30] However, due to the non-equilibrium nature of PLD growth, where supersaturation and film growth occur sequentially, there are still variations in cation composition depending on processing parameters such as working distance and laser spot size on the target.[31] These effects are amplified in sputtering processes because negative ions (O^{2-}) backsputter onto the deposited thin films and change the cation stoichiometry. This has been overcome by employing 90° off-axis sputtering,[32] producing high quality films over large areas. However, sputtering is still more challenging for rapid growth of a wide range of TMOs. Molecular Beam Epitaxy (MBE) is a powerful technique to fabricate thin films and heterostructures of TMOs. However, the cation composition is solely dependent on how accurately each flux of source material is controlled. Conventional *in situ* techniques, such as a quartz crystal microbalance (QCM), reflection high-energy electron diffraction (RHEED), and atomic absorption spectroscopy (AAS), can give controllability of each flux within 0.1%–1%.[33] This can be converted into point defect densities of $\sim 10^{20}/cm^3$, which is far below the defect level in conventional semiconductors.

In order to accurately control the cation stoichiometry to less than 0.1%, a fabrication process governed by thermodynamics is required. Adsorption-controlled growth is one typical example of this, where complex compounds can be grown only when one element is supplied, and vapor phases are stable at certain growth conditions otherwise. This growth technique was originally used for GaAs growth due to the high volatility of As but has since expanded to the growth of oxides such as SnO[34] and $PbTiO_3$ [Fig. 2(a)].[35] For adsorption-controlled growth, however, one element in the compound must be volatile in order to create a growth window for both practical growth and pressure regions [Fig. 2(b)].[36] Hence, the hybrid growth technique has been developed, in which a metalorganic precursor is used as a source in a conventional physical vapor deposition (PVD) process. Details of the hybrid growth method will be discussed later.

IV. DEFECTS IN OXIDE FILMS IN RELATION TO STRAIN LEVELS

While the means to controlling the oxygenation level and cation composition are clear, if not always straightforward, the problems of strain are more complex. First, it is noted that, since functional properties of TMOs depend strongly on the metal–oxygen bond length,[37] interfacial strain presents additional problems in oxide devices over conventional semiconductor devices.

Second, it is noted that strain cannot be easily eliminated simply by choosing a lattice-matched substrate since there are limited substrates available and also because the ultimate-goal substrate, Si, has a very different lattice size/structure to oxides. We also note that a great deal of research has been dedicated to growing oxides on Si, success having been achieved by growing $SrTiO_3$ buffers on Si by MBE[38,39] and, more recently, by PLD,[40] allowing subsequent growth of high quality epitaxial oxides by a range of methods.[41] Recent years, meanwhile, have seen the use of amorphous phase epitaxy (APE) and vertically aligned nanocomposites (VAN) to deposit high-quality oxide thin films on Si, along with many studies on MBE.[42–48]

A key problem for strained epitaxial films is the inability to readily relax the film/substrate interfacial strain.[49–52] Consequently, *additional* deleterious defects occur compared to comparative bulk materials.[52] Figure 3 and the panel below it give a guide to the defects which form because of substrate-induced strain in a typical perovskite epitaxial film.

In fact, the defect landscape in epitaxial oxide thin films, how and why the different defects form and how they evolve with thickness, has been little studied. This is partly because of new and exciting functionalities emerging in TMOs every few years and the focus is then on understanding the new science originating from them. On the other hand, if more perfect films could be made, a whole new class of high performance oxide devices would result, and a broad electronics oxide application area would surely take off quite rapidly.

As detailed in Fig. 3, a key problem for epitaxial oxide films is that poor kinetics (arising from the high melting points of oxides) limits the formation of strain-relieving misfit dislocations. It could be argued that misfit dislocations are preferable to the variety of "other" strain-relieving defects which form in their place in regions 1 and 2. This is because the physical properties of oxides are intimately linked to structure. Thus, while misfit dislocations have their disordered dislocation cores localized *near the*

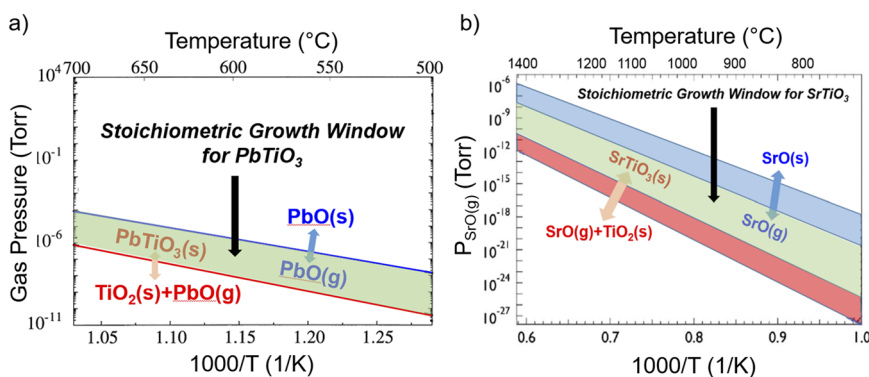**FIG. 2.** (a) Equilibrium curves for two reactions governing adsorption-controlled growth of $PbTiO_3$ [reproduced with permission from Theis *et al.*, Thin Solid Films **325**(1-2), 107–114 (1998). Copyright 1998 Elsevier]. (b) Calculated MBE growth window for $SrTiO_3$ using solid metal sources [reproduced with permisssion from Jalan *et al.*, Appl. Phys. Lett. **95**(3), 032906 (2009). Copyright 2009 AIP Publishing LLC].[36]
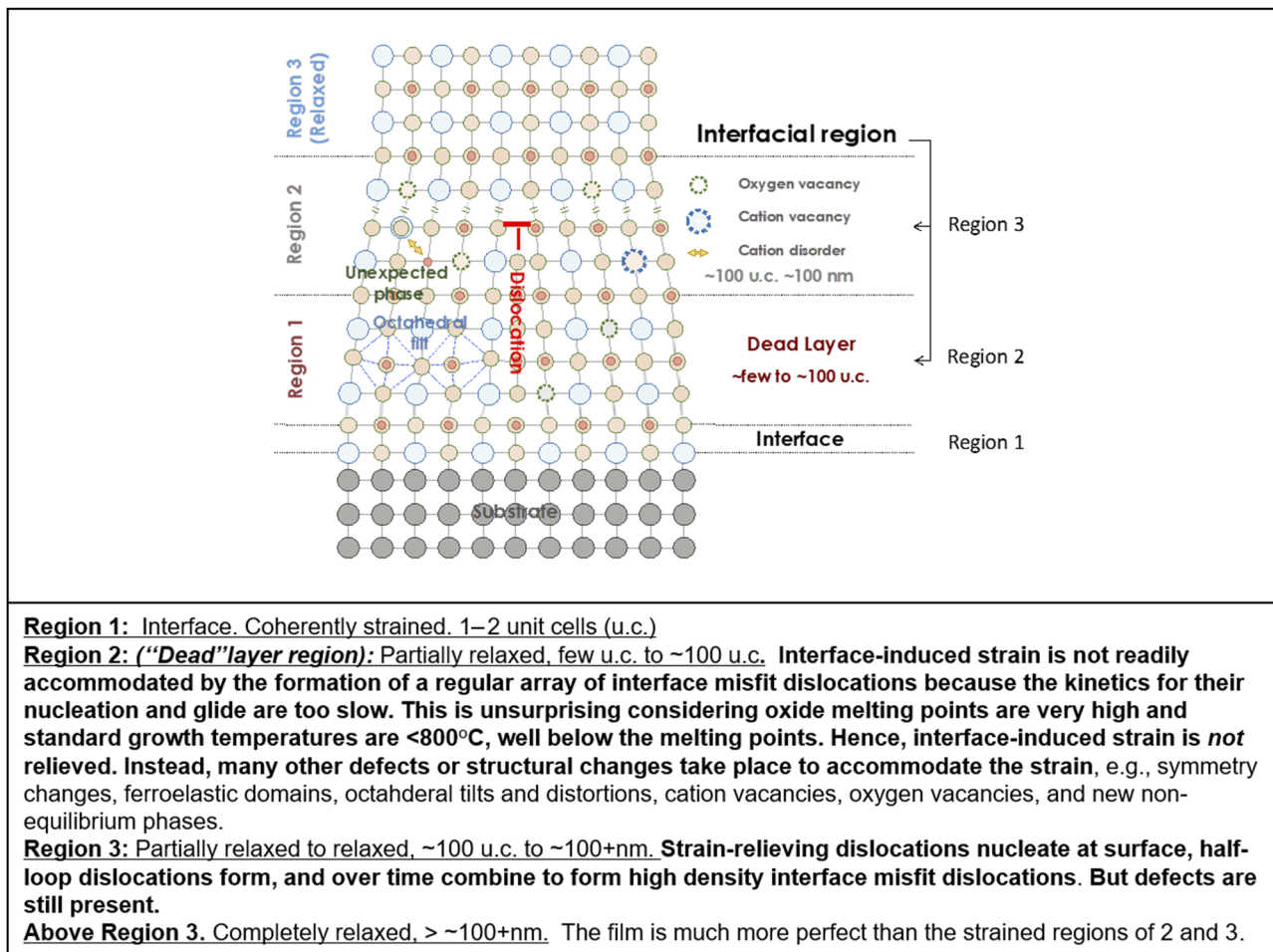
Region 1: Interface. Coherently strained. 1–2 unit cells (u.c.)

Region 2: ("Dead" layer region): Partially relaxed, few u.c. to ~100 u.c. **Interface-induced strain is not readily accommodated by the formation of a regular array of interface misfit dislocations because the kinetics for their nucleation and glide are too slow. This is unsurprising considering oxide melting points are very high and standard growth temperatures are <800°C, well below the melting points. Hence, interface-induced strain is *not* relieved. Instead, many other defects or structural changes take place to accommodate the strain**, e.g., symmetry changes, ferroelastic domains, octahderal tilts and distortions, cation vacancies, oxygen vacancies, and new non-equilibrium phases.

Region 3: Partially relaxed to relaxed, ~100 u.c. to ~100+nm. **Strain-relieving dislocations nucleate at surface, half-loop dislocations form, and over time combine to form high density interface misfit dislocations. But defects are still present.**

Above Region 3. Completely relaxed, > ~100+nm. The film is much more perfect than the strained regions of 2 and 3.

FIG. 3. Schematic of typical standard, epitaxial TMO film. Defects in different regions of standard film are described in the panel.[31,51–54]

interface with the substrate, the "other" defects are located *within and throughout the body of the film*. Hence, these "other" defects degrade the structure and properties *within the film*, not just at the interface.

While high temperature growth/annealing (to at least 1000 °C) can give sufficient kinetics for the desired high density

interface misfit dislocation formation, enhanced crystallinity films[53] and enhanced properties,[54,55] such high temperatures cause other serious problems, as detailed in Fig. 4. A key question is how to reduce defects in complex oxide and how to do this at practical growth temperatures in relatively simply ways.
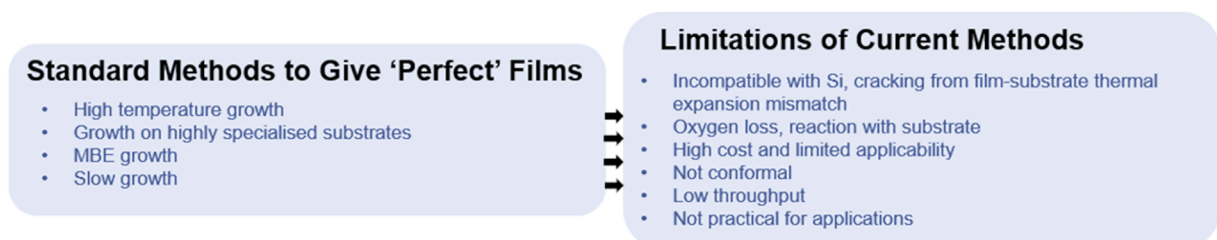

FIG. 4. Current, recent, and new approaches for achieving highly more perfect transition metal oxide thin films, as well as limitations of current methods.

V. METHODS TO IMPROVE OXIDE FILM PERFECTION AT PRACTICAL GROWTH TEMPERATURES

We highlight eight possible emerging approaches for engineering more perfect complex oxide films. The methods are at different stages of understanding/development, some being at very early stage but showing tantalizing property enhancements to warrant much deeper investigation. (A) adsorption-controlled growth by MBE; (B) hybrid growth processes, i.e., PLD + soft chemical; (C) interval growth in PLD; (D) amorphous phase epitaxy (APE), (E) liquid assisted growth, (F) vertically aligned nanocomposites, and (G) laser-heated substrates with localized high

temperature heating. A rough comparison of the methods is given in Table I.

A. Adsorption-controlled growth by MBE

Accurate composition control is one of the most vexing challenges to the growth of complex oxide films, including perovskites. A commonly touted advantage of PLD and sputtering is that the composition of the target is accurately transferred to the film. This is only an approximation; due to the angular dependence of the species leaving the target, the composition delivered to the film is, in general, not the same as that of the target.[31,56]

TABLE I. Advantages and disadvantages of modified or new methods for improving perfection in oxide thin films.

Method	Advantages	Disadvantages
(A) Adsorption-controlled growth by MBE	Easy by PLD. Automatic composition control provided by thermodynamics.	Not easily possible by non-PLD deposition. When growing a heterostructure containing multiple materials, the adsorption-controlled growth windows of all of the materials may not overlap at a common substrate temperature, complicating the synthesis.
(B) Hybrid growth process	Enables highly stoichiometric films.	Limitation of metalorganic source. High vapor pressure is required. Liquid phase near room temperature is preferred.
(C) Interval growth in PLD	Improves film homogeneity and crystallinity without reducing growth rate.	Will not enhance "beneficial" dislocation formation as diffusion is not enhanced but may still reduce point defect formation. May not allow growth temperatures to be significantly reduced.
(D) Amorphous phase epitaxy	Relatively straightforward.	Films can be susceptible to stacking faults during growth. Method largely unexplored for improving film perfection.
(E) Liquid assisted growth	Easy by a wide range of vapor deposition methods. For equivalent levels perfection, cf. standard methods, enables significant reduction in growth temperature. Very rapid growth (with 1 μm/min) standard, i.e., more than an order of magnitude faster than other methods. Single-crystal like quality.	Melt resides on film surface after growth and needs to be removed. Not all film compositions have accessible eutectics.
(F) Vertically aligned nanocomposites	Easy to grow by vapor methods. Demonstrated strongly enhanced functionalities in many functional oxides.	Need to find compatible materials which grow together in a phase separated manner in the composite. One of the phases in the composite may not provide a function beyond enabling higher film crystalline quality.
(G) Laser-heated substrates with localized high temperature heating	With T_{sub} up to 2000 °C demonstrated, *in situ* termination of atomically smooth substrates with chemically specific surfaces is now possible. Pinpointing the heat to just the substrate decreases contamination and enables the growth of refractory oxides having low vapor pressures with unparalleled perfection.	Requires specialized hardware.

The non-stoichiometric incident flux results in defects in the growing film.

Accurate composition control is also a difficult challenge for the growth of multicomponent oxide films by MBE, with one important exception. The exception is for the growth of oxides with a volatile constituent, analogous to the growth of GaAs and other compound semiconductors by MBE.[57,58] It is for such compounds that the MBE technique was developed and shown to work incredibly well.[59–64] It might seem surprising that it is easier to control the composition of a material containing a volatile constituent, the loss of which depends sensitively on the substrate temperature used. The reason it works is because for many materials a thermodynamic "growth window" exists where the volatile constituent can be supplied in excess and thermodynamics automatically limits the amount of the volatile constituent that gets incorporated into the growing film.[57,58,63,64] In simplistic terms, the arriving arsenic only sticks if it can bond to gallium; the As–As bond is much weaker than the As–Ga bond causing the excess arsenic to desorb. Provided that the growth window is sufficiently large, a significant excess of the volatile component can be provided and films of uniform composition can be achieved despite temperature variations across the substrate. Growth with such automatic composition control, provided by thermodynamics, is referred to as adsorption-controlled growth.

The first complex oxide perovskite for which adsorption-controlled growth was demonstrated was the growth of $PbTiO_3$ by metalorganic chemical vapor deposition (MOCVD) [Fig. 2(a)].[65] Since then, adsorption-controlled growth has been widely applied to the growth of oxides by MBE. Specifically, $PbTiO_3$,[66] $Bi_2Sr_2CuO_6$,[67] $Bi_4Ti_3O_{12}$,[35,68,69] $BiFeO_3$,[42,70–72] $BiMnO_3$,[73] $BiVO_4$,[74] EuO,[75,76] $LuFe_2O_4$,[77] $SrRuO_3$,[78,79] Sr_2RuO_4,[80,81] Ba_2RuO_4,[80] $CaRuO_3$,[79] Ba_2IrO_4,[82] $SrIrO_3$,[83] Sr_2IrO_4,[83] $BaSnO_3$,[84] SnO,[34] and Sr_3SnO[85] have all been grown under adsorption-controlled conditions by MBE. Additional complex oxides—$SrTiO_3$,[86] $GdTiO_3$,[87] $BaTiO_3$,[88] $CaTiO_3$,[89] $LaVO_3$,[90] $(La,Sr)VO_3$,[91] $BaSnO_3$,[92] and $SrSnO_3$[93]

—have been grown under adsorption-controlled conditions utilizing volatile metalorganic precursors, i.e., by MOMBE.[94,95] While adsorption-controlled growth enables single-phase complex oxide perovskite films to be readily and reproducibly prepared, how close the resulting films are to being stoichiometric depends on how far the single-phase region extends in the direction of the volatile constituent that is supplied in excess during growth. This variation with temperature is used to control the point defect concentrations of compound semiconductors during post-growth annealing.[96] Only when this single-phase region ends at the stoichiometric composition of the compound will the films produced be precisely stoichiometric. Thus, adsorption-controlled growth conditions are not synonymous with perfect composition control.

Nevertheless, adsorption-controlled growth has enabled complex oxide perovskites of the highest quality, judged by their structural and electronic properties, to be produced by MBE. Several examples are listed in Table II together with the best films reported by non-MBE thin film growth methods. In most cases, the perfection achieved in these films exceeds that of the very best bulk single crystals of these same materials.

B. Hybrid growth

As mentioned earlier, for achieving adsorption-controlled growth, compounds need a volatile element, such as As in GaAs[23] or PbO in $PbTiO_3$.[35] However, there are no adsorption-controlled growth conditions at practical substrate temperatures for other general oxides, such as $SrTiO_3$. In order to overcome such barriers, hybrid MBE processes have been developed by Stemmer's group.[86] They found a growth window for stoichiometric $SrTiO_3$ films by using Sr metal and titanium tetraisopropoxide (TTIP) gas as source materials (Fig. 5). In addition, La-doped $SrTiO_3$ films by hybrid MBE exhibited high mobilities of ~32 000 cm^2 V^{-1} s^{-1} (unstrained, at 1.8 K)[109] and ~128 000 cm^2 V^{-1} s^{-1} (strained, at 1.8 K),[110] which are higher than those of doped $SrTiO_3$ single crystals.[111] In addition

TABLE II. Comparison of the best transport properties reported on films made by oxide MBE vs other thin film growth techniques.

| Material	Best MBE figure of merit	Best non-MBE figure of merit	References
EuO	Metal-insulator transition $\Delta R/R = 10^{11}$	Metal-insulator transition $\Delta R/R = 5 \times 10^4$	97 and 98
ZnO	$\mu_e = 230\,000$ cm^2/(V s) at 1 K	$\mu_e = 5500$ cm^2/(V s) at 1 K	99 and 100
SrRuO$_3$	$R_{300\,K}/R_{10\,K} = 115$	$R_{300\,K}/R_{10\,K} = 14$	101
Sr$_2$RuO$_4$	Superconducting $T_{c,midpoint} = 1.8$ K	Superconducting $T_{c,midpoint} = 0.8$ K	81 and 102
SrTiO$_3$	$\mu_e = 53\,200$ cm^2/(V s) at 2 K	$\mu_e = 6600$ cm^2/(V s) at 2 K	9 and 103
SrVO$_3$	$R_{300\,K}/R_{5\,K} = 222$	$R_{300\,K}/R_{5\,K} = 2$	104 and 105
SrSnO$_3$	$\mu_e = 70$ cm^2/(V s) at 300 K	$\mu_e = 40$ cm^2/(V s) at 300 K	106 and 107
BaSnO$_3$	$\mu_e = 183$ cm^2/(V s) at 300 K	$\mu_e = 140$ cm^2/(V s) at 300 K	84 and 108
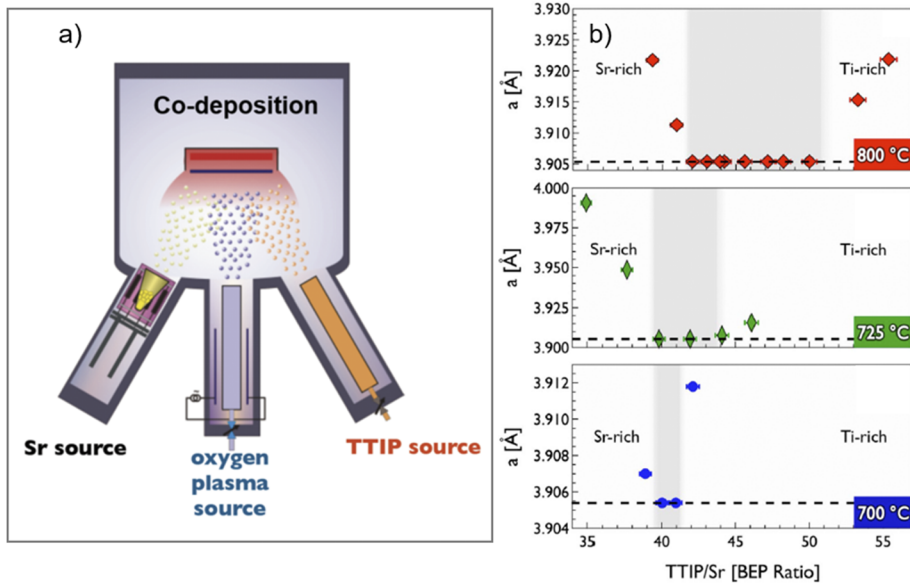
FIG. 5. Adsorption controlled MBE growth. (a) Schematic of a hybrid MBE system incorporating TTIP sources. Reproduced with permission from Jalan *et al.* (2020). Copyright 2020 Jalan *et. al.*[165] (b) Stoichiometric growth window for SrTiO3 in hybrid MBE. Reproduced with permission from Jalan *et al.*, Appl. Phys. Lett. **95**(3), 032906 (2009).[36]

to SrTiO$_3$, this hybrid MBE technique has been extended to other materials systems, such as BaSnO$_3$[112] and SrVO$_3$.[113]

Stemming from the success of an MBE-based hybrid growth technique, Eom's group developed a PLD-based hybrid technique. In this work, laser ablation of a single crystal SrO target occurs simultaneously with the addition of TTIP into the chamber (Fig. 6), enabling adsorption-controlled growth of SrTiO$_3$ films. This PLD-based hybrid growth technique is expected to be applicable to a wide variety of material systems because it can be easily combined with existing PLD systems to produce various types of heterostructures. For the evaporation in the MBE-based technique, effusion cells should be used to control the flux of element accurately. The use of effusion cells is limited by the melting temperature of materials. However, a pulsed laser can evaporate stable compounds of which
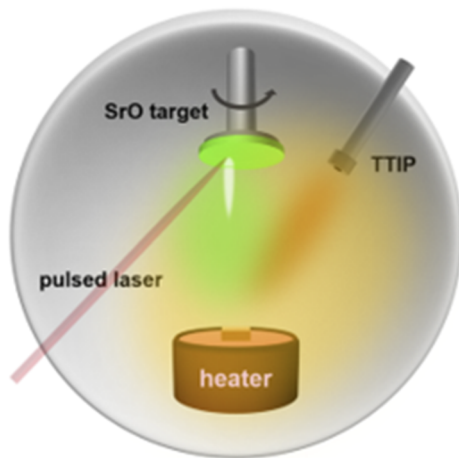
melting temperature is very high, such as SrO. Thus, hybrid PLD can provide an additional choice of materials in complex oxide thin film growth. There is, therefore, much potential for this method to be applied to other TMOs with one volatile element, e.g., Ga, Sn, Bi, Zn, or Ru based perovskites.

C. Interval growth

Interval growth involves cycles of a PLD "burst" to form high density nuclei of single atomic layer thickness, followed by relaxation annealing with only short diffusion distances between nuclei.[12,114] It leads to a more homogeneous mixing of species (Fig. 7) and greater control of volatile species (e.g., Bi), which become trapped in the film rather than evaporating during the time required to build up the film thickness.[115] It has been explored before mainly for growth of films along step edges in vicinal substrates, giving step-flow growth to produce very smooth, chemically uniform *ultrathin* films.[12] It has also been used for creating high energy storage dielectric films with record energy densities,[115] as well as double perovskite films which are hard to order the cations during normal growth.[116,117] In summary, interval growth *effectively* enhances kinetics and enables better film stoichiometry and also does so for relatively thick films.

D. Amorphous phase epitaxy

For PLD and sputtering, defects in films arising from the high kinetic energy of impinging species during growth and UV irradiation from the PLD plume are challenging to mitigate entirely.[118,119] By crystallizing amorphous films on a single crystal substrate, amorphous phase epitaxy (APE), also known as solid phase epitaxy (SPE), avoids many of the defect formation mechanisms associated with PLD. It has, therefore, been widely used for the fabrication of semiconductor materials, typically highly intolerant to defects. On the other hand, factors such as mismatched atomic configurations
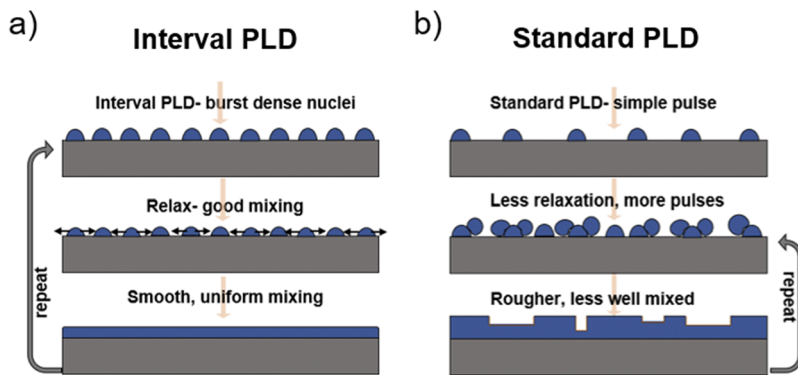

FIG. 6. Schematic of hybrid PLD.

FIG. 7. Schematic of (a) interval growth used in pulsed laser deposition for control of film stoichiometry and crystallinity and (b) standard pulsed laser deposition process.

at the amorphous/crystalline (a/c) interface can lead to stacking faults.[120]

Although the majority of APE studies focus on semiconductor materials, defect formations in STO have been explored.[43,121–125] The crystallization of STO on both STO (001) and SiO_2/Si (001) substrates has been studied. While epitaxial growth is observed on STO, the SiO_2/Si (001) substrate acts as a mask rather than a template for crystallization, favoring polycrystalline growth. Meanwhile, in both cases, highly defective layers are attributed to nucleation away from the a/c interface at high temperatures (>600 °C). On the other hand, lower temperatures enable the synthesis of single crystalline oxides in nanoscale geometries, enabling the a/c interface to propagate over relatively large distances (up to ~2 μm demonstrated, so far), while avoiding polycrystalline nucleation.[43] This is in agreement with previous work by Wang et al., in which the defect levels present in STO films are characterized by Rutherford backscattering as a function of annealing temperature.[123] Oxygen vacancies in $EuTiO_3$ films grown by APE have also been correlated with the dielectric constant by Shimamoto et al.[126] and, in STO, to x-ray photoelectron spectroscopy (XPS) spectra by Norga et al.[122] X-ray coherent diffraction imaging and x-ray ptychography have also been proposed as potential defect characterization techniques.[125]

Other reports have demonstrated crystallization of $EuTiO_3$, $CaTiO_3$, $SmNiO_3$, and $PrAlO_3$ by APE. For non-perovskite oxides, VO_2, V_2O_3, Cr_2O_3, and beta-Bi_2O_3 have been successfully grown by APE. This highlights the applicability of the technique to a wide range of oxide materials.[126–132] To our knowledge, there is no direct comparison between defect concentrations in films fabricated by PLD and by APE, but it is clear from existing research that APE provides a promising route to the development of low defect level oxide thin films.

E. Liquid assisted growth

It is possible to use thin liquid layers to give very high crystallinity and also growth rates of epitaxial TMO films. The method is a form of liquid phase epitaxy and is termed hybrid liquid phase epitaxy or tri-phase epitaxy.[133,134] It has been studied widely for rapid growth of the superconductor, $REBa_2Cu_3O_{7-x}$ (REBCO, where RE = rare earth). A schematic of the generalized process is shown in Fig. 8. In the method, a molten eutectic liquid (~1 μm) is first deposited on a single crystal substrate. Then, a vapor phase of species of the film to be grown (derived from a target material in a vacuum) is applied to the surface of the film. The species diffuse through the melt, and the film nucleates and grows epitaxially on the substrate surface. The liquid then moves to the film surface as the film thickens.

The basis of this method has resulted in an industry process for cost-effective production of long length $YBa_2Cu_3O_7$ (YBCO) conductors.[135–139] For YBCO, defects are required for flux pinning and can be induced by delivering the vapor species rapidly to the liquid surface. For most other functional oxide films, very low defect concentrations can be easily engineered since the films grow in a single-crystal-like manner under low supersaturation. The method
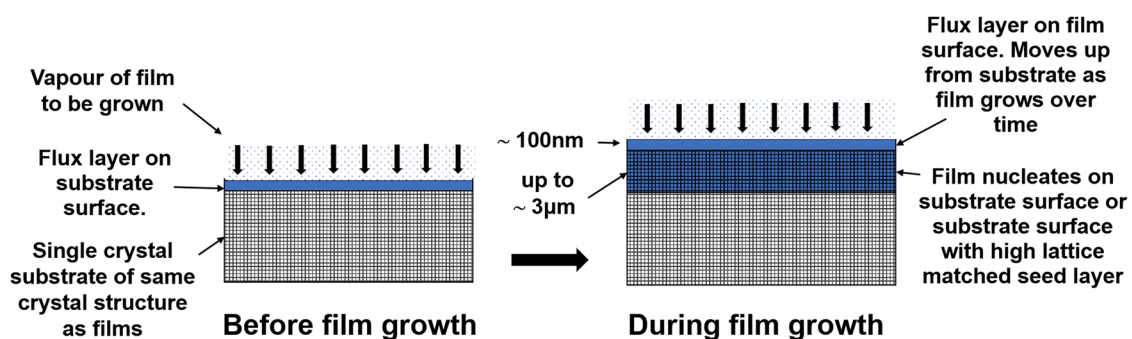

FIG. 8. Schematic of hybrid liquid phase epitaxy (or tri-phase epitaxy growth process).

has also been demonstrated for BiFeO₃, using a Bi–Fe–O eutectic liquid (Bi:Fe ratio ~ 5.8),[140] for delafossite CuScO₂ using a Bi–O flux.[141] In the non-oxide area, GaAs has grown from a Bi solvent.[142]

F. Vertically aligned nanocomposites

Vertically aligned epitaxial nanocomposite (VAN) films are a relatively new form of epitaxial thin film structure giving rise to a new epitaxy paradigm.[143–147] With appropriate selection of very stiff second phase nanopillar materials, the structures can enable highly crystalline films to be made with very uniform strain which remains constant with film thickness. Uniform, controlled strain is important not only for defect control in TMOs but also for ensuring that the bulk properties can be "dialled-in" to the film, which is very often not the case for plain, standard TMO films.

Strain uniformity in VAN films occurs because strain is controlled by very finely spaced (~20 nm to 30 nm pitch) vertical nanopillars which control the strain vertically, preventing relaxation vertically. This contrasts with the single substrate interface which the film "loses sight of" as it grows thicker. The $La_{0.9}Ba_{0.1}MnO_3$ (LBMO) system serves as an ideal exemplar to demonstrate the excellent uniformity and control of strain in a VAN film, cf. a standard plain film. This is because LBMO (similar to other manganites) exhibits several structural pseudo-cubic distortions, the formation of each one depending sensitively on the strain level. Since the strain relaxes gradually as films grow, the different phases of LBMO form as the films thicken. Figure 9(a) shows the example

of ~45 nm thick plain LBMO films (where A and A′ denote the tetragonal phase and T shows the twinning phase) compared to the same thickness VAN LBMO films (with only one homogeneous tetragonal phase). The VAN composition is 50% LBMO +50% MgO. We observe several LBMO phases for the LBMO plain film, cf. a single uniform phase for the VAN BMO film. The uniform strain has enabled the bulk ferromagnetic insulating properties of LBMO films to be realized in VAN which cannot be achieved in plain films.[148]

We note that for the *same* overall film growth rate, self-assembled vertical interfaces in the VAN films grow orders of magnitude more slowly than planar film/substrate interfaces in standard films (over 10s of minutes, cf. seconds). This will strongly impact the functional properties of the different interfaces, and more work is needed to understand these comparative properties. Aside from the LBMO system, other key examples of much improved properties resulting from the enhanced perfection in VAN films compared to plain films include enhanced magnetization in $La_{1-x}Sr_xMnO_3$ (LSMO),[150] very strongly enhanced polarization and reduced leakage in oxide ferroelectric systems, e.g., BaTiO₃-based[147,151–153] and BiFeO₃,[154] > 2 order of magnitude enhanced ionic conductivity in CeO₂ and $(Y_2O_3)_{0.08}(ZrO_2)_{0.92}$ (YSZ) [as show in Fig. 9(b)].[149,155,156]

G. Laser-heated substrates

The use of lasers is a burgeoning trend in the growth of transition metal oxide thin films. Lasers are, of course, an essential
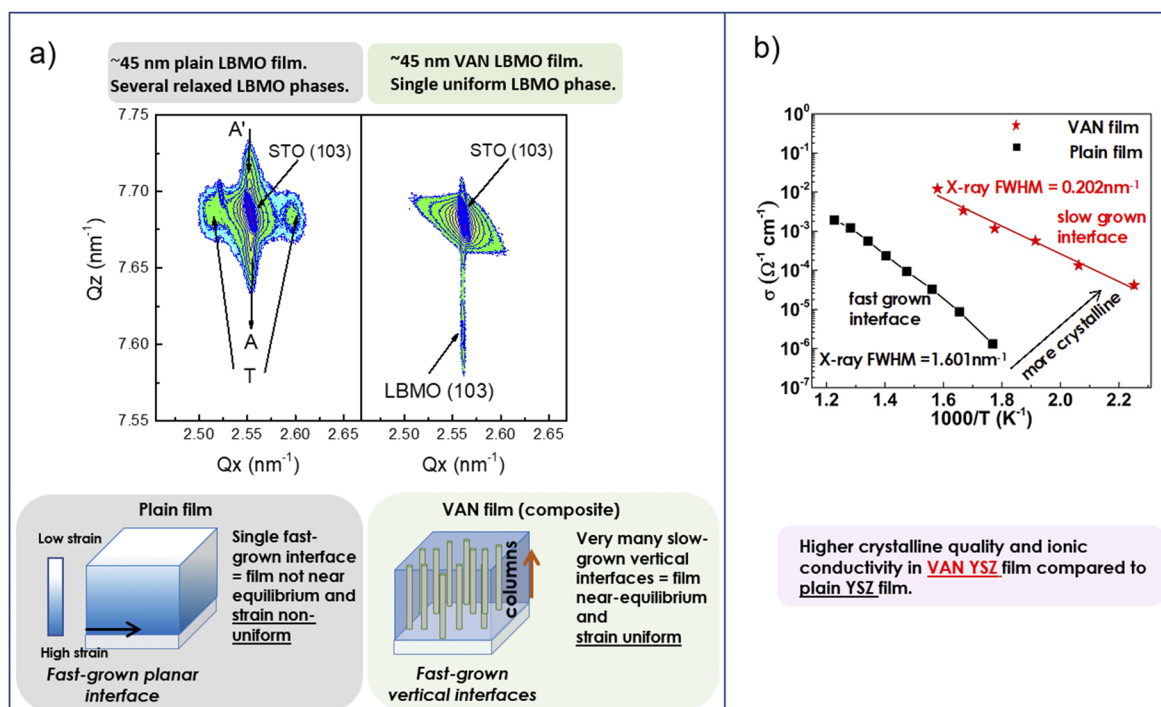

FIG. 9. Improved strain and crystallinity of self-assembled VAN thin films and consequent improved functional properties. (a) X-ray reciprocal space maps around the SrTiO₃ (103) peak comparing plain LBMO films to VAN (LBMO + MgO) films grown on SrTiO₃. (b) Ionic conductivity of plain YSZ films compared to VAN (YSZ + SrTiO₃) films. Adapted from Ref. 148.
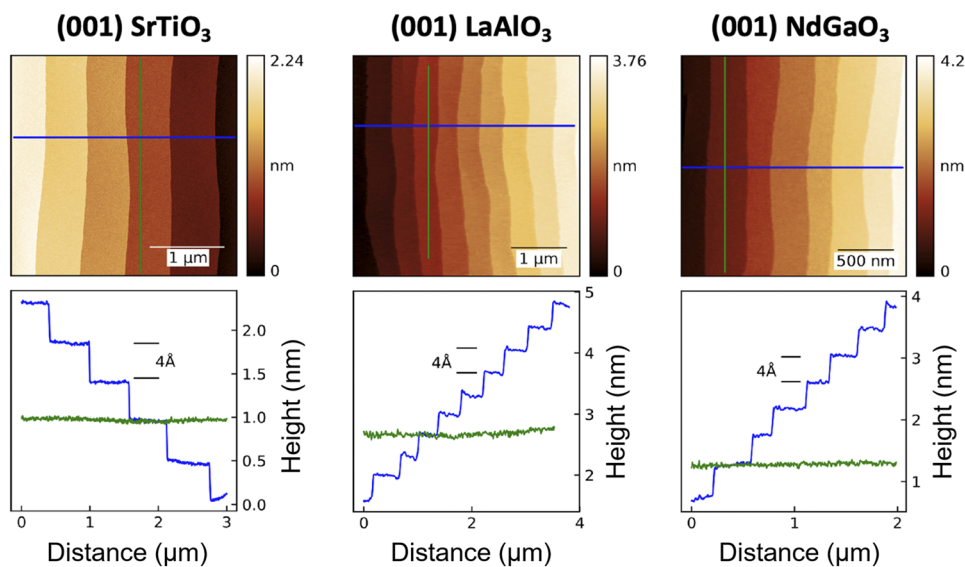
FIG. 10. Atomically smooth substrates with chemically specific surfaces produced by *in situ* laser heating. Starting from commercially polished substrates, a 1 K/s ramp, 200 s soak at a temperature and oxygen partial pressure that optimized for each type of substrate, and rapid cooling cycle is applied yielding the surface morphologies revealed by the AFM images and height profiles along the blue and green lines in the AFM images. Reproduced with permission from Jäger *et al.*, Appl. Phys. Lett. **112**(11), 111601 (2018). Copyright 2018 AIP Publishing LLC.[160]

ingredient of PLD. Beyond PLD, lasers are being used to heat substrates[157–160] and even to provide stable thermal evaporation sources.[161] It is this former application of lasers that is particularly empowering. New materials and better ways to make materials are enabled by expanding synthesis space—the range of conditions that can be used for film growth. Lasers enable higher temperatures, higher heating and cooling rates, higher oxygen pressures because oxidation of the heating elements is no longer an issue when there are no heating elements, less outgassing from parts in and around the heater because the beam can be shaped and applied with surgical precision to just the desired region, and more reliable transition metal oxide thin film deposition systems because there are fewer failure points in the system and the laser is outside the vacuum chamber.

An example of the benefit of laser-heated substrates is shown in Fig. 10. The quality of the smooth and chemically specific termination that has been achieved by Jochen Mannhart's group at the Max Planck Institute for Solid State Research[160] is as good or better than what has been achieved by *ex situ* chemical etching and annealing procedures.[162,163] This laser-heated procedure, however, has additional benefits of safety and simplicity. The starting substrate is as-received from the commercial vendor where it received a traditional chemomechanical polish. As all oxide substrates absorb well at the 10.6 μm wavelength of a CO_2 laser due to their phonons, no backside coating or special preparation (and potential contamination) of the substrate is needed. No acids and associated safety risks are involved in the termination process. The process is quick and has been demonstrated to work for every binary oxide substrate attempted, however, for ternary oxides suitable conditions have only been found for select compounds.[164] So far, the substrates that can be terminated with atomic smoothness like the examples shown in Fig. 10 include SrTiO₃, LaAlO₃, NdGaO₃, MgO, Al₂O₃, DyScO₃, and TbScO₃.[108,160] Following this quick thermal preparation step, the atomically terminated surface is in the growth chamber and ready for deposition. Film growth can then immediately proceed over a broad range or temperature (T_{sub} up to 2000 °C has

been demonstrated) and heating/cooling rates.[164] The ability to efficiently heat just the substrate decreases contamination and enables the growth of refractory oxides possessing low vapor pressures with unparalleled perfection. These many significant advantages of laser-heated substrates are already yielding significant property improvements in transition metal oxide thin films.[108]

VI. CONCLUSIONS

In conclusion, considering both the enormous potential offered by complex transition metal epitaxial films across all fields of electronics and their limited applications uptake after more than 30 years of study, often because thin film properties cannot replicate what is achieved in bulk, we have considered ways to improve crystalline perfection. We have reviewed emerging and new avenues of research at different stages of understanding and development, which could move the field in a positive direction to better quality films using new methodologies, including adsorption-controlled growth by MBE, interval growth in PLD, hybrid growth processes, amorphous phase epitaxy, liquid assisted growth, vertically aligned nanocomposite films, and finally, laser-heating of substrates with localized high temperature heating. The new decade of 2020 is the right time for oxide enthusiasts to focus on improving the perfection of oxide thin films, prompted by the methods outlined in this perspective. In this way, the enormous promise of functional transition metal oxides can be harnessed to enable lower power devices.

ACKNOWLEDGMENTS

REFERENCES

[1] P. Ganguly and C. N. R. Rao, J. Solid State Chem. **53**(2), 193–216 (1984).

[2] C. N. R. Rao and B. Raveau, Acc. Chem. Res. **22**(3), 106–113 (1989).

[3] C. N. R. Rao, Annu. Rev. Phys. Chem. **40**, 291–326 (1989).

[4] R. Mahendiran, S. K. Tiwary, A. K. Raychaudhuri, T. V. Ramakrishnan, R. Mahesh, N. Rangavittal, and C. N. R. Rao, Phys. Rev. B **53**(6), 3348–3358 (1996).

[5] A. M. dos Santos, S. Parashar, A. R. Raju, Y. S. Zhao, A. K. Cheetham, and C. N. R. Rao, Solid State Commun. **122**(1-2), 49–52 (2002).

[6] C. N. R. Rao, MRS Bull. **43**(3), 220–226 (2018).

[7] L. Schmidt-Mende and J. L. MacManus-Driscoll, Mater. Today **10**(5), 40–48 (2007).

[8] J.-Y. Ha, J.-W. Choi, C.-Y. Kang, S. F. Karmanenko, D. J. Choi, S.-J. Yoon, and H.-J. Kim, J. Electroceram. **17**(2-4), 141–144 (2006).

[9] Y. Kozuka, Y. Hikita, C. Bell, and H. Y. Hwang, Appl. Phys. Lett. **97**(1), 012107 (2010).

[10] D. Keeble, S. Wicklein, L. Jin, C. Jia, W. Egger, and R. Dittmann, Phys. Rev. B **87**(19), 195409 (2013).

[11] C.-H. Lee, N. D. Orloff, T. Birol, Y. Zhu, V. Goian, E. Rocas, R. Haislmaier, E. Vlahos, J. A. Mundy, L. F. Kourkoutis, Y. Nie, M. D. Biegalski, J. Zhang, M. Bernhagen, N. A. Benedek, Y. Kim, J. D. Brock, R. Uecker, X. X. Xi, V. Gopalan, D. Nuzhnyy, S. Kamba, D. A. Muller, I. Takeuchi, J. C. Booth, C. J. Fennie, and D. G. Schlom, Nature **502**(7472), 532 (2013).

[12] D. H. A. Blank, M. Dekkers, and G. Rijnders, J. Phys. D: Appl. Phys. **47**(3), 034006 (2014).

[13] D. G. Schlom, L.-Q. Chen, X. Pan, A. Schmehl, and M. A. Zurbuchen, J. Am. Ceram. Soc. **91**(8), 2429–2454 (2008).

[14] A. Ohtomo and H. Y. Hwang, Nature **427**(6973), 423–426 (2004).

[15] Deloitte, *Semiconductors: The Next Wave Opportunities and Winning Strategies for Semiconductor Companies* (Deloitte, Beijing, 2019), p. 5.

[16] J. Chakhalian, A. J. Millis, and J. Rondinelli, Nat. Mater. **11**(2), 92–94 (2012).

[17] J. Yu, L. Dong, B. Peng, L. Yuan, Y. Huang, L. Zhang, Y. Zhang, and R. Jia, J. Alloys Compd. **821**(8), 153532 (2020).

[18] M. E. Ayhan, M. Shinde, B. Todankar, P. Desai, A. K. Ranade, M. Tanemura, and G. Kalita, Mater. Lett. **262**(5), 127074 (2020).

[19] Y.-M. Chen, C.-H. Wu, K.-M. Chang, Y.-X. Zhang, N. Xu, T.-Y. Yu, and A. Chin, J. Nanosci. Nanotechnol. **20**(7), 4110–4113 (2020).

[20] S. Goedecker, T. Deutsch, and L. Billard, Phys. Rev. Lett. **88**(23), 235501 (2002).

[21] H.-S. Lee, T. Mizoguchi, T. Yamamoto, S.-J. L. Kang, and Y. Ikuhara, Acta Mater. **55**(19), 6535–6540 (2007).

[22] J. L. Richards, Nature **177**(4500), 182–183 (1956).

[23] L. Pfeiffer and K. West, Physica E **20**(1-2), 57–64 (2003).

[24] W. D. Kingery, *Introduction to Ceramics* (John Wiley & Sons, New York, 1976).

[25] M. G. Blamire, J. L. MacManus-Driscoll, N. D. Mathur, and Z. H. Barber, Adv. Mater. **21**(38-39), 3827–3839 (2009).

[26] R. N. Basu and H. S. Maiti, Trans. Indian Ceram. Soc. **47**(6), 176–179 (1988).

[27] J. Dho, X. Qi, H. Kim, J. L. MacManus-Driscoll, and M. G. Blamire, Adv. Mater. **18**(11), 1445–1448 (2006).

[28] J. H. Song, T. Susaki, and H. Y. Hwang, Adv. Mater. **20**(13), 2528 (2008).

[29] D. O. Scanlon, Phys. Rev. B **87**(16), 161201 (2013).

[30] R. Eason, *Pulsed Laser Deposition of Thin Films: Applications-LED Growth of Functional Materials* (John Wiley & Sons, New York, 2007).

[31] T. Ohnishi, K. Shibuya, T. Yamamoto, and M. Lippmaa, J. Appl. Phys. **103**(10), 103703 (2008).

[32] C. B. Eom, J. Z. Sun, K. Yamamoto, A. F. Marshall, K. E. Luther, T. H. Geballe, and S. S. Laderman, Appl. Phys. Lett. **55**(6), 595–597 (1989).

[33] D. G. Schlom, J. H. Haeni, J. Lettieri, C. D. Theis, W. Tian, J. C. Jiang, and X. Q. Pan, Mater. Sci. Eng.: B **87**(3), 282–291 (2001).

[34] A. B. Mei, L. Miao, M. J. Wahila, G. Khalsa, Z. Wang, M. Barone, N. J. Schreiber, L. E. Noskin, H. Paik, and T. E. Tiwald, Phys. Rev. Mater. **3**(10), 105202 (2019).

[35] C. D. Theis, J. Yeh, D. G. Schlom, M. Hawley, and G. Brown, Thin Solid Films **325**(1-2), 107–114 (1998).

[36] B. Jalan, P. Moetakef, and S. Stemmer, Appl. Phys. Lett. **95**(3), 032906 (2009).

[37] P. G. Radaelli, M. Marezio, H. Y. Hwang, S.-W. Cheong, and B. Batlogg, Phys. Rev. B **54**(13), 8992–8995 (1996).

[38] B. T. Liu, K. Maki, Y. So, V. Nagarajan, R. Ramesh, J. Lettieri, J. H. Haeni, D. G. Schlom, W. Tian, X. Q. Pan, F. J. Walker, and R. A. McKee, Appl. Phys. Lett. **80**(25), 4801–4803 (2002).

[39] J. Q. He, C. L. Jia, V. Vaithyanathan, D. G. Schlom, J. Schubert, A. Gerber, H. H. Kohlstedt, and R. H. Wang, J. Appl. Phys. **97**(10), 104921 (2005).

[40] D. Diaz-Fernandez, M. Spreitzer, T. Parkelj, and D. Suvorov, Appl. Surf. Sci. **455**, 227–235 (2018).

[41] C. Merckling, M. Korytov, U. Celano, M.-H. M. Hsu, S. M. Neumayer, S. Jesse, and S. de Gendt, J. Vac. Sci. Technol., A **37**(2), 021510 (2019).

[42] R. Ramesh, R. Uecker, W. A. Doolittle, P. Reiche, Z.-K. Liu, M. Bernhagen, W. Tian, J. F. Ihlefeld, and D. G. Schlom, *Adsorption-Controlled Growth of BiFeO₃ by MBE and Integration with Wide Band Gap Semiconductors* (Sandia National Laboratories, Alberquerque, 2008).

[43] Y. Chen, J. A. Tilka, Y. Ahn, J. Park, A. Pateras, T. Zhou, D. E. Savage, I. McNulty, M. V. Holt, D. M. Paskiewicz, D. D. Fong, T. F. Kuech, and P. G. Evans, J. Phys. Chem. C **123**(12), 7447–7456 (2019).

[44] V. Vaithyanathan, J. Lettieri, W. Tian, A. Sharan, A. Vasudevarao, Y. L. Li, A. Kochhar, H. Ma, J. Levy, P. Zschack, and J. C. Woicik, J. Appl. Phys. **100**(9), 024108 (2006).

[45] L. Mazet, S. M. Yang, S. V. Kalinin, S. Schamm-Chardon, and C. Dubourdieu, Sci. Technol. Adv. Mater. **16**(20), 036005 (2015).

[46] M. P. Warusawithana, C. Cen, C. R. Sleasman, J. C. Woicik, Y. Li, L. F. Kourkoutis, J. A. Klug, H. Li, P. Ryan, L.-P. Wang, M. Bedzyk, D. A. Muller, L.-Q. Chen, J. Levy, and D. G. Schlom, Science **324**(5925), 367–370 (2009).

[47] J. Huang, A. Gellatly, A. Kauffmann, X. Sun, and H. Wang, Cryst. Growth Des. **18**(8), 4388–4394 (2018).

[48] D. H. Kim, S. Ning, and C. A. Ross, J. Mater. Chem. C **7**(30), 9128–9148 (2019).

[49] T. Suzuki, Y. Nishi, and M. Fujimoto, Philos. Mag. A **79**(10), 2461–2483 (1999).

[50] J. L. Maurice, F. Pailloux, A. Barthelemy, O. Durand, D. Imhoff, R. Lyonnet, A. Rocher, and J. P. Contour, Philos. Mag. **83**(28), 3201–3224 (2003).

[51] H. Boschker, J. Kautz, E. P. Houwman, W. Siemons, D. H. A. Blank, M. Huijben, G. Koster, A. Vailionis, and G. Rijnders, Phys. Rev. Lett. **109**(15), 157207 (2012).

[52] F. Sandiumenge, J. Santiso, L. Balcells, Z. Konstantinovic, J. Roqueta, A. Pomar, J. Pedro Espinos, and B. Martinez, Phys. Rev. Lett. **110**(10), 107206 (2012).

[53] L. S.-J. Peng, X. X. Xi, B. H. Moeckly, and S. P. Alpay, Appl. Phys. Lett. **83**(22), 4592–4594 (2003).

[54] H. P. Sun, X. Q. Pan, J. H. Haeni, and D. G. Schlom, Appl. Phys. Lett. **85**(11), 1967–1969 (2004).

[55] O. Shapoval, S. Hühn, J. Verbeeck, M. Jungbauer, A. Belenchuk, and V. Moshnyaga, J. Appl. Phys. **113**(17), 17C711 (2013).

[56] T. Ohnishi, M. Lippmaa, T. Yamamoto, S. Meguro, and H. Koinuma, Appl. Phys. Lett. **87**(24), 241919 (2005).

[57] K. Günther, Z. Naturforsch., A **13**(12), 1081–1089 (1958).

[58] H. Freller and K. G. Günther, Thin Solid Films **88**(4), 291–307 (1982).

[59] J. R. Arthur, Jr., J. Appl. Phys. **39**(8), 4032–4034 (1968).

[60] A. Y. Cho, Surf. Sci. **17**, 494–503 (1969).

[61] A. Y. Cho, J. Appl. Phys. **41**(7), 2780–2786 (1970).

[62] A. Y. Cho, J. Appl. Phys. **42**(5), 2074–2081 (1971).

[63] H. Seki and A. Koukitu, J. Cryst. Growth **78**(2), 342–352 (1986).

[64] J. Y. Tsao and J. P. Harbison, Phys. Today **46**(10), 125 (1993).

[65]G. Dormans, P. Van Veldhoven, and M. De Keijser, J. Cryst. Growth **123**(3-4), 537–544 (1992).

[66]C. D. Theis and D. G. Schlom, J. Cryst. Growth **174**(1-4), 473–479 (1997).

[67]S. Migita, Y. Kasai, H. Ota, and S. Sakai, Appl. Phys. Lett. **71**(25), 3712–3714 (1997).

[68]C. D. Theis, J. Yeh, D. G. Schlom, M. E. Hawley, G. W. Brown, J. C. Jiang, and X. Q. Pan, Appl. Phys. Lett. **72**(22), 2817–2819 (1998).

[69]S. Migita, H. Ota, H. Fujino, Y. Kasai, and S. Sakai, J. Cryst. Growth **200**(1-2), 161–168 (1999).

[70]J. Kabelac, S. Ghosh, P. Dobal, and R. Katiyar, J. Vac. Sci. Technol., B **25**(3), 1049–1052 (2007).

[71]J. F. Ihlefeld, A. Kumar, V. Gopalan, D. G. Schlom, Y. B. Chen, X. Q. Pan, T. Heeg, J. Schubert, X. Ke, P. Schiffer, J. Orenstein, L. W. Martin, Y. H. Chu, and R. Ramesh, Appl. Phys. Lett. **91**(7), 071922 (2007).

[72]E. H. Smith, J. F. Ihlefeld, C. A. Heikes, H. Paik, Y. Nie, C. Adamo, T. Heeg, Z.-K. Liu, and D. G. Schlom, Phys. Rev. Mater. **1**(2), 023403 (2017).

[73]J. H. Lee, X. Ke, R. Misra, J. F. Ihlefeld, X. S. Xu, Z. G. Mei, T. Heeg, M. Roeckerath, J. Schubert, and Z. K. Liu, J. L. Musfeldt, P. Schiffer, and D. G. Schlom, Appl. Phys. Lett. **96**(26), 262905 (2010).

[74]S. Stoughton, M. Showak, Q. Mao, P. Koirala, D. A. Hillsberry, S. Sallis, L. F. Kourkoutis, K. Nguyen, L. F. J. Piper, D. A. Tenne, N. J. Podraza, D. A. Muller, C. Adamo, and D. G. Schlom, APL Mater. **1**(4), 042112 (2013).

[75]R. W. Ulbricht, A. Schmehl, T. Heeg, J. Schubert, and D. G. Schlom, Appl. Phys. Lett. **93**(10), 102105 (2008).

[76]R. Sutarto, S. G. Altendorf, B. Coloru, M. Moretti Sala, T. Haupricht, C. F. Chang, Z. Hu, C. Schussler-Langeheine, N. Hollmann, H. Kierspel, H. H. Hsieh, H. J. Lin, C. T. Chen, and L. H. Tjeng, Phys. Rev. B **79**(20), 205318 (2009).

[77]C. M. Brooks, R. Misra, J. A. Mundy, L. A. Zhang, B. S. Holinsworth, K. R. O'Neal, T. Heeg, W. Zander, J. Schubert, J. L. Musfeldt, Z.-K. Liu, D. A. Muller, P. Schiffer, and D. G. Schlom, Appl. Phys. Lett. **101**(13), 132907 (2012).

[78]D. Shai, C. Adamo, D. Shen, C. M. Brooks, J. Harter, E. J. Monkman, B. Burganov, D. G. Schlom, and K. M. Shen, Phys. Rev. Lett. **110**(8), 087004 (2013).

[79]H. P. Nair, Y. Liu, J. P. Ruf, N. J. Schreiber, S.-L. Shang, D. J. Baek, B. H. Goodge, L. F. Kourkoutis, Z.-K. Liu, K. M. Shen, and D. G. Schlom, APL Mater. **6**(4), 046101 (2018).

[80]B. Burganov, C. Adamo, A. Mulder, M. Uchida, P. King, J. Harter, D. Shai, A. Gibbs, A. Mackenzie, and R. Uecker, Phys. Rev. Lett. **116**(19), 197003 (2016).

[81]H. P. Nair, J. P. Ruf, N. J. Schreiber, L. Miao, M. L. Grandon, D. J. Baek, B. H. Goodge, J. P. C. Ruff, L. F. Kourkoutis, K. M. Shen, and D. G. Schlom, APL Mater. **6**(10), 101108 (2018).

[82]M. Uchida, Y. Nie, P. King, C. Kim, C. Fennie, D. Schlom, and K. Shen, Phys. Rev. B **90**(7), 075142 (2014).

[83]Y. F. Nie, P. King, C. Kim, M. Uchida, H. Wei, B. D. Faeth, J. Ruf, J. Ruff, L. Xie, and X. Pan, Phys. Rev. Lett. **114**(1), 016401 (2015).

[84]H. Paik, Z. Chen, E. Lochocki, A. Seidner H., A. Verma, N. Tanen, J. Park, M. Uchida, S. Shang, B.-C. Zhou, M. Brützam, R. Uecker, Z.-K. Liu, D. Jena, K. M. Shen, D. A. Muller, and D. G. Schlom, APL Mater. **5**(11), 116107 (2017).

[85]Y. Ma, A. Edgeton, H. Paik, B. Faeth, C. Parzyck, B. Pamuk, S.-L. Shang, Z. K. Liu, K. M. Shen, D. G. Schlom, and C. B. Eom, "Realization of epitaxial thin films of the topological crystalline insulator Sr_3SnO" (submitted).

[86]B. Jalan, R. Engel-Herbert, N. J. Wright, and S. Stemmer, J. Vac. Sci. Technol., A **27**(3), 461–464 (2009).

[87]P. Moetakef, J. Y. Zhang, S. Raghavan, A. P. Kajdos, and S. Stemmer, J. Vac. Sci. Technol., A **31**(4), 041503 (2013).

[88]Y. Matsubara, K. S. Takahashi, Y. Tokura, and M. Kawasaki, Appl. Phys. Express **7**(12), 125502 (2014).

[89]R. C. Haislmaier, E. D. Grimley, M. D. Biegalski, J. M. LeBeau, S. Trolier-McKinstry, V. Gopalan, and R. Engel-Herbert, Adv. Funct. Mater. **26**(40), 7271–7279 (2016).

[90]H.-T. Zhang, L. R. Dedon, L. W. Martin, and R. Engel-Herbert, Appl. Phys. Lett. **106**(23), 233102 (2015).

[91]M. Brahlek, L. Zhang, H.-T. Zhang, J. Lapano, L. R. Dedon, L. W. Martin, and R. Engel-Herbert, Appl. Phys. Lett. **109**(10), 101903 (2016).

[92]A. Prakash, P. Xu, X. Wu, G. Haugstad, X. Wang, and B. Jalan, J. Mater. Chem. C **5**(23), 5730–5736 (2017).

[93]T. Wang, L. R. Thoutam, A. Prakash, W. Nunn, G. Haugstad, and B. Jalan, Phys. Rev. Mater. **1**(6), 061601 (2017).

[94]K. Endo, S. Saya, S. Misawa, and S. Yoshida, Thin Solid Films **206**(1-2), 143–145 (1991).

[95]L. L. H. King, K. Y. Hsieh, D. J. Lichtenwalner, and A. I. Kingon, Appl. Phys. Lett. **59**, 3045–3047 (1991).

[96]D. Hurle, J. Appl. Phys. **107**(12), 121301 (2010).

[97]D. V. Averyanov, O. E. Parfenov, A. M. Tokmachev, I. A. Karateev, O. A. Kondratev, A. N. Taldenkov, M. S. Platunov, F. Wilhelm, A. Rogalev, and V. G. Storchak, Nanotechnology **29**(19), 195706 (2018).

[98]T. Yamasaki, K. Ueno, A. Tsukazaki, T. Fukumura, and M. Kawasaki, Appl. Phys. Lett. **98**(8), 082116 (2011).

[99]J. Falson, Y. Kozuka, M. Uchida, J. H. Smet, T.-h. Arima, A. Tsukazaki, and M. Kawasaki, Sci. Rep. **6**, 26598 (2016).

[100]A. Tsukazaki, A. Ohtomo, T. Kita, Y. Ohno, H. Ohno, and M. Kawasaki, Science **315**(5817), 1388–1391 (2007).

[101]D. Kan, R. Aso, H. Kurata, and Y. Shimakawa, J. Appl. Phys. **113**(17), 173912 (2013).

[102]Y. Krockenberger, M. Uchida, K. S. Takahashi, M. Nakamura, M. Kawasaki, and Y. Tokura, Appl. Phys. Lett. **97**(8), 082502 (2010).

[103]T. A. Cain, A. P. Kajdos, and S. Stemmer, Appl. Phys. Lett. **102**(18), 182101 (2013).

[104]J. A. Moyer, C. Eaton, and R. Engel-Herbert, Adv. Mater. **25**(26), 3578–3582 (2013).

[105]W. C. Sheets, B. Mercey, and W. Prellier, Appl. Phys. Lett. **91**(19), 192102 (2007).

[106]T. Truttmann, A. Prakash, J. Yue, T. E. Mates, and B. Jalan, Appl. Phys. Lett. **115**(15), 152103 (2019).

[107]E. Baba, D. Kan, Y. Yamada, M. Haruta, H. Kurata, Y. Kanemitsu, and Y. Shimakawa, J. Phys. D: Appl. Phys. **48**(45), 455106 (2015).

[108]A. P. Nono Tchiomo, W. Braun, B. P. Doyle, W. Sigle, P. van Aken, J. Mannhart, and P. Ngabonziza, APL Mater. **7**(4), 041119 (2019).

[109]J. Son, P. Moetakef, B. Jalan, O. Bierwagen, N. J. Wright, R. Engel-Herbert, and S. Stemmer, Nat. Mater. **9**(6), 482 (2010).

[110]B. Jalan, S. J. Allen, G. E. Beltz, P. Moetakef, and S. Stemmer, Appl. Phys. Lett. **98**(13), 132102 (2011).

[111]A. Spinelli, M. Torija, C. Liu, C. Jan, and C. Leighton, Phys. Rev. B **81**(15), 155110 (2010).

[112]A. Prakash, J. Dewey, H. Yun, J. S. Jeong, K. A. Mkhoyan, and B. Jalan, J. Vac. Sci. Technol., A **33**(6), 060608 (2015).

[113]M. Brahlek, L. Zhang, C. Eaton, H.-T. Zhang, and R. Engel-Herbert, Appl. Phys. Lett. **107**(14), 143108 (2015).

[114]D. H. A. Blank, G. Koster, G. Rijnders, E. van Setten, P. Slycke, and H. Rogalla, J. Cryst. Growth **211**(1-4), 98–105 (2000).

[115]A. Kursumovic, W. Li, S. Cho, P. Curran, D. H. L. Tjhe, and J. L. MacManus-Driscoll, Nano Energy **71**, 104536 (2020).

[116]C. Grygiel, S. R. C. McMitchell, Z. Xu, L. Yan, H. J. Niu, D. Giap, J. Bacsa, P. R. Chalker, and M. J. Rosseinsky, Chem. Mater. **22**(6), 1955–1957 (2010).

[117]S. Chakraverty, A. Ohtomo, and M. Kawasaki, Appl. Phys. Lett. **97**(24), 243107 (2010).

[118]F. Baiutti, G. Christiani, and G. Logvenov, Beilstein J. Nanotechnol. **5**, 596–602 (2014).

[119]F. V. E. Hensling, D. J. Keeble, J. Zhu, S. Brose, C. Xu, F. Gunkel, S. Danylyuk, S. S. Nonnenmann, W. Egger, and R. Dittmann, Sci. Rep. **8**(1), 8846 (2018).

[120]T. Motooka, K. Nisihira, S. Munetoh, K. Moriguchi, and A. Shintani, Phys. Rev. B **61**(12), 8537–8540 (2000).

[121]Y. Chen, M. H. Yusuf, Y. Guan, R. Jacobson, M. G. Lagally, S. E. Babcock, T. F. Kuech, and P. G. Evans, ACS Appl. Mater. Interfaces **9**(46), 41034–41042 (2017).

[122]G. J. Norga, C. Marchiori, C. Rossel, A. Guiller, J. P. Locquet, H. Siegwart, D. Caimi, J. Fompeyrine, J. W. Seo, and C. Dieker, J. Appl. Phys. **99**(8), 084102 (2006).

[123]F. Wang, M. Badaye, Y. Yoshida, and T. Morishita, Nucl. Instrum. Methods Phys. Res., Sect. B **118**(1-4), 547–551 (1996).

[124]M. N. K. Bhuiyan, H. Kimura, T. Tambo, and C. Tatsuyama, Jpn. J. Appl. Phys. Part 1 **43**(11B), 7879–7880 (2004).

[125]P. G. Evans, Y. Chen, J. A. Tilka, S. E. Babcock, and T. F. Kuech, Curr. Opin. Solid State Mater. Sci. **22**(6), 229–242 (2018).

[126]K. Shimamoto, Y. Hirose, S. Nakao, T. Fukumura, and T. Hasegawa, J. Cryst. Growth **378**, 243–245 (2013).

[127]C. W. White, L. A. Boatner, P. S. Sklad, C. J. McHargue, J. Rankin, G. C. Farlow, and M. J. Aziz, Nucl. Instrum. Methods Phys. Res., Sect. B **32**(1-4), 11–22 (1988).

[128]J. Shi, Y. Zhou, and S. Ramanathan, Nat. Commun. **5**(1), 4860 (2014).

[129]W. L. I. Waduge, Y. Chen, P. Zuo, N. Jayakodiarachchi, T. F. Kuech, S. E. Babcock, P. G. Evans, and C. H. Winter, ACS Appl. Nano Mater. **2**(11), 7449–7458 (2019).

[130]A. Matsuda, Y. Nozawa, S. Kaneko, and M. Yoshimoto, Appl. Surf. Sci. **480**, 956–961 (2019).

[131]A. G. Bagmut and I. A. Bagmut, J. Cryst. Growth **517**, 68–71 (2019).

[132]Z. Sun, D. Oka, and T. Fukumura, Cryst. Growth Des. **19**(12), 7170–7174 (2019).

[133]A. Kursumovic, R. I. Tomov, R. Hühne, J. L. MacManus-Driscoll, B. A. Glowacki, and J. E. Evetts, Supercond. Sci. Technol. **17**(10), 1215–1223 (2004).

[134]K. S. Yun, B. D. Choi, Y. Matsumoto, J. H. Song, N. Kanda, T. Itoh, M. Kawasaki, T. Chikyow, P. Ahmet, and H. Koinuma, Appl. Phys. Lett. **80**(1), 61–63 (2002).

[135]J. L. Macmanusdriscoll, J. C. Bravman, and R. B. Beyers, Physica C **241**(3-4), 401–413 (1995).

[136]B. Maiorov, A. Kursumovic, L. Stan, H. Zhou, H. Wang, L. Civale, R. Feenstra, and J. L. MacManus-Driscoll, Supercond. Sci. Technol. **20**(9), S223–S229 (2007).

[137]J. L. MacManus-Driscoll, M. Bianchetti, A. Kursumovic, G. Kim, W. Jo, H. Wang, J. H. Lee, G. W. Hong, and S. H. Moon, APL Mater. **2**(8), 086103 (2014).

[138]J. W. Lee, J. H. Lee, S. H. Moon, and S. I. Yoo, Prog. Supercond. Cryog. **14**(4), 28–31 (2012).

[139]M. R. Beasley and R. H. Hammond, *Stanford In Situ High Rate YBCO Process: Transfer to Metal Tapes and Process Scale Up* (Stanford University, Stanford, CA, 2009).

[140]M. Li, A. Kursumovic, X. Qi, and J. L. MacManus-Driscoll, J. Cryst. Growth **293**(1), 128–135 (2006).

[141]Y. Matsubara, T. Makino, C. Chen, S. Tsukimoto, K. Ueno, Y. Kozuka, Y. Ikuhara, and M. Kawasaki, Appl. Phys. Express **5**(1), 011201 (2012).

[142]S. Saravanan, K. Jeganathan, K. Baskar, T. Jimbo, T. Soga, and M. Umeno, J. Cryst. Growth **192**(1-2), 23–27 (1998).

[143]B. N. Zhu, G. Schusteritsch, P. Lu, J. L. MacManus-Driscoll, and C. J. Pickard, APL Mater. **7**(6), 061105 (2019).

[144]X. Sun, J. L. MacManus-Driscoll, and H. Wang, "Spontaneous ordering of oxide-oxide epitaxial vertically aligned nanocomposite thin films," Annu. Rev. Mater. Sci. (to be published) (2019).

[145]J. L. MaCmanus-Driscoll, P. Zerrer, H. Wang, H. Yang, J. Yoon, A. Fouchet, R. Yu, M. G. Blamire, and Q. Jia, Nat. Mater. **7**(4), 314–320 (2008).

[146]J. L. MacManus-Driscoll, Adv. Funct. Mater. **20**(13), 2035–2045 (2010).

[147]S. A. Harrington, J. Zhai, S. Denev, V. Gopalan, H. Wang, Z. Bi, S. A. T. Redfern, S.-H. Baek, C. W. Bark, C.-B. Eom, Q. Jia, M. E. Vickers, and J. L. MacManus-Driscoll, Nat. Nanotechnol. **6**(8), 491–495 (2011).

[148]C. Yun, E. Choi, M. W. Li, X. Sun, T. Maity, R. Wu, J. Jian, S. Xue, S. Cho, H. Wang, and J. L. MacManus-Driscoll, "Achieving the bulk properties of perovskite manganites in thin films," Nanoscale (to be published) (2019).

[149]S. Lee, W. Zhang, F. Khatkhatay, H. Wang, Q. Jia, and J. L. MacManus-Driscoll, Nano Lett. **15**(11), 7362–7369 (2015).

[150]A. Chen, Z. Bi, C.-F. Tsai, J. Lee, Q. Su, X. Zhang, Q. Jia, J. L. MacManus-Driscoll, and H. Wang, Adv. Funct. Mater. **21**(13), 2423–2429 (2011).

[151]O. Lee, S. A. Harrington, A. Kursumovic, E. Defay, H. Wang, Z. Bi, C.-F. Tsai, L. Yan, Q. Jia, and J. L. MacManus-Driscoll, Nano Lett. **12**(8), 4311–4317 (2012).

[152]O. Lee, A. Kursumovic, Z. X. Bi, C. F. Tsai, H. Y. Wang, and J. L. MacManus-Driscoll, Adv. Mater. Interfaces **4**(15), 1700336 (2017).

[153]A. L. Sangle, O. J. Lee, A. Kursumovic, W. Zhang, A. Chen, H. Wang, and J. L. MacManus-Driscoll, Nanoscale **10**(7), 3460–3468 (2018).

[154]H. Yang, H. Wang, G. F. Zou, M. Jain, N. A. Suvorova, D. M. Feldmann, P. C. Dowden, R. F. DePaula, J. L. MacManus-Driscoll, A. J. Taylor, and Q. X. Jia, Appl. Phys. Lett. **93**(14), 142904 (2008).

[155]S. Lee, W. Zhang, F. Khatkhatay, Q. Jia, H. Wang, and J. L. MacManus-Driscoll, Adv. Funct. Mater. **25**(27), 4328–4333 (2015).

[156]S. M. Yang, S. Lee, J. Jian, W. Zhang, P. Lu, Q. Jia, H. Wang, T. W. Noh, S. V. Kalinin, and J. L. MacManus-Driscoll, Nat. Commun. **6**(1), 8588 (2015).

[157]P. E. Dyer, A. Issa, P. H. Key, and P. Monk, Supercond. Sci. Technol. **3**(9), 472–475 (1990).

[158]K. H. Wu, C. L. Lee, J. Y. Juang, T. M. Uen, and Y. S. Gou, Appl. Phys. Lett. **58**(10), 1089–1091 (1991).

[159]S. Ohashi, M. Lippmaa, N. Nakagawa, H. Nagasawa, H. Koinuma, and M. Kawasaki, Rev. Sci. Instrum. **70**(1), 178–183 (1999).

[160]M. Jäger, A. Teker, J. Mannhart, and W. Braun, Appl. Phys. Lett. **112**(11), 111601 (2018).

[161]W. Braun and J. Mannhart, AIP Adv. **9**(8), 085310 (2019).

[162]A. Biswas, C.-H. Yang, R. Ramesh, and Y. H. Jeong, Prog. Surf. Sci. **92**(2), 117–141 (2017).

[163]N. Wadehra, R. Tomar, R. K. Gopal, Y. Singh, S. Dattagupta, and S. Chakraverty, "Planar Hall effect and anisotropic magnetoresistance in a polar-polar interface of LaVO3-KTaO3 with strong spin-orbit coupling," Nat. Commun. **11**, 874 (2020).

[164]W. Braun, private communication (2020).

[165]Jalan *et al.*, see https://www.mrl.ucsb.edu/~stemmer/main_pdfs/SpinAps_workshop_short.pdf for "Two-dimensional electron gas in SrTiO$_3$," (2020).